

# Effective Treatment of Low-Grade Myofibroblastic Sarcoma with Apatinib: A Case Report and Literature Review

Yan Lin<sup>1,\*</sup>, Xing Gao<sup>1,\*</sup>, Ziyu Liu<sup>1</sup>, Zhihui Liu<sup>1</sup>, Yongqiang Li<sup>1</sup>, Rong Liang<sup>1</sup>, Zhiling Liao<sup>2</sup>, Jiazhou Ye<sup>3</sup>

<sup>1</sup>Department of Medical Oncology, Guangxi Medical University Cancer Hospital, Nanning, Guangxi, People's Republic of China; <sup>2</sup>Department of Pathology, Guangxi Medical University Cancer Hospital, Nanning, Guangxi, People's Republic of China; <sup>3</sup>Department of Hepatobiliary Surgery, Guangxi Medical University Cancer Hospital, Nanning, Guangxi, People's Republic of China

\*These authors contributed equally to this work

Correspondence: Rong Liang, Department of Medical Oncology, Guangxi Medical University Cancer Hospital, Nanning, Guangxi, 530021, People's Republic of China, Tel +86 771 5335155, Fax +86 771 5335155, Email liangrong@gxmu.edu.cn; Jiazhou Ye, Department of Hepatobiliary Surgery, Guangxi Medical University Cancer Hospital, Nanning, Guangxi, 530021, People's Republic of China, Tel +86 771 5331211, Fax +86 771 5331211, Email yejiazhou@gxmu.edu.cn

**Abstract:** Low-grade myofibroblastic sarcoma (LGMS) is a rare, poorly differentiated, malignant tumor. The disease mainly occurs in the head and neck and rarely metastasizes at any age. Currently, there is no consensus regarding the treatment of metastatic LGMS. Here, we report the case of a 45-year-old man who was admitted to our hospital with cough for two weeks and abdominal pain for one week. Preoperative computed tomography revealed a large mass (116×35 mm) in both the lungs and jejunal mass (maximum diameter, 32 mm). The tumor was excised, and immunohistochemical staining was positive for SMA and CD117 and negative for desmin and CD34, indicating a case of LGMS. The patient was effectively treated with apatinib (250 mg/day) after failure of imatinib, liposomal doxorubicin, and ifosfamide. The progression-free survival time was 8.5 months, and the overall survival time was 17 months after treatment with apatinib. No grade 3 or 4 side effects were observed, except hand-foot syndrome. Whole-exome sequencing (WES) and RNA sequencing (RNA-seq) were performed on the patient's jejunal tumor and para-cancerous tissue samples, and bioinformatics analysis was performed on the results. WES identified five mutations in MKI67, OR2J2, EPPK1, FCGBP, and OR10G4. RNA-seq revealed that 1422 genes were upregulated and 1890 genes were downregulated. The differentially expressed genes were mainly enriched in the phosphatidylinositol 3-kinase (PI3K) signaling pathway, neuroactive ligand-receptor interaction signaling pathway, and cAMP signaling pathway. Our study indicated that apatinib may be a potential novel and effective treatment for LGMS.

**Keywords:** low-grade myofibroblastic sarcoma, apatinib, VEGFR-PI3K/Akt signaling pathway, whole-exome sequencing, RNA sequencing

## Introduction

Low-grade myofibroblastic sarcoma (LGMS) is a rare sarcoma tumor, and according to the data, only 103 cases have been reported from 1998 to 2019.<sup>1</sup> Mentz et al first described LGMS in 1998 as a tumor with myofibroblastic differentiation.<sup>2</sup> LGMS is an atypical tumor composed of myofibroblasts, which are spindle-shaped mesenchymal cells present in almost every soft tissue.<sup>3</sup> It presents as a slow-growing, painless mass, and is often mistaken for a benign lesion. LGMS occurs most often in adults and predominantly in men of an average age of 40 years (age range: 9–75 years).<sup>4,5</sup> Painless mass enlargement is its typical clinical manifestation, and patients may also experience fever, chills, and leukocytosis.<sup>6</sup> LGMS is mainly located in deep soft tissues and occasionally grows in connective tissue gaps, muscle or bone in an irregular infiltration pattern. The diagnosis of LGMS primarily relies on postoperative histological examinations. Histopathologically, LGMS consists of fusiform cells arranged in sheet-like or storiform patterns. The tumor cells have constricted slender nuclei with amphophilic or eosinophilic cytoplasm. The fusiform nuclei of tumor cells have a low mitotic rate and mild nuclear pleomorphism.

Immunohistochemistry showed that tumor cells expressed muscle-specific actin,  $\alpha$ -smooth muscle actin, fibronectin, desmin, calcineurin, and vimentin, but not S100, CK, CD34, EMA, or laminin. The ki67 marking index was between 8% and 45%.<sup>6-8</sup> Surgery is currently the primary treatment for LGMS. However, the standardization of its treatment, including surgery, chemotherapy, and radiotherapy, requires further research because of the rarity of reported cases.

Here, we present a case of multifocal LGMS that co-occurred in the lung and abdominal cavity. The patient was effectively treated with apatinib after failure of imatinib, liposomal doxorubicin, and ifosfamide. Whole-exome sequencing (WES) and RNA sequencing (RNA-seq) was used to pinpoint genetic mutations that could be associated with this rare disease; and to the best of our knowledge, this is the first reported case of LGMS that responded well to apatinib.

## Case Report

### Medical History

On February 19, 2017, a 45-year-old man was admitted to the Guangxi Medical University Cancer Hospital complaining of abdominal pain and cough for two weeks. An Eastern Cooperative Oncology Group performance status (ECOG PS) score of 4 and numerical rating scale score of 5 were given. A physical examination revealed a solid mass around the umbilicus. It measured 20×30 mm, was ill-defined, and irregular. Laboratory tests revealed a serum carbohydrate antigen (CA125) level of 231.2 U/mL. The serum levels of total bilirubin, prothrombin time, international normalized ratio, albumin, platelet count, creatinine, CA199, and CEA were within normal limits. A computed tomography (CT) scan of the patient's chest revealed large masses in both lungs, enlarged mediastinal lymph nodes, left pleural effusion, pulmonary artery main, and branch embolism (Figure 1A).

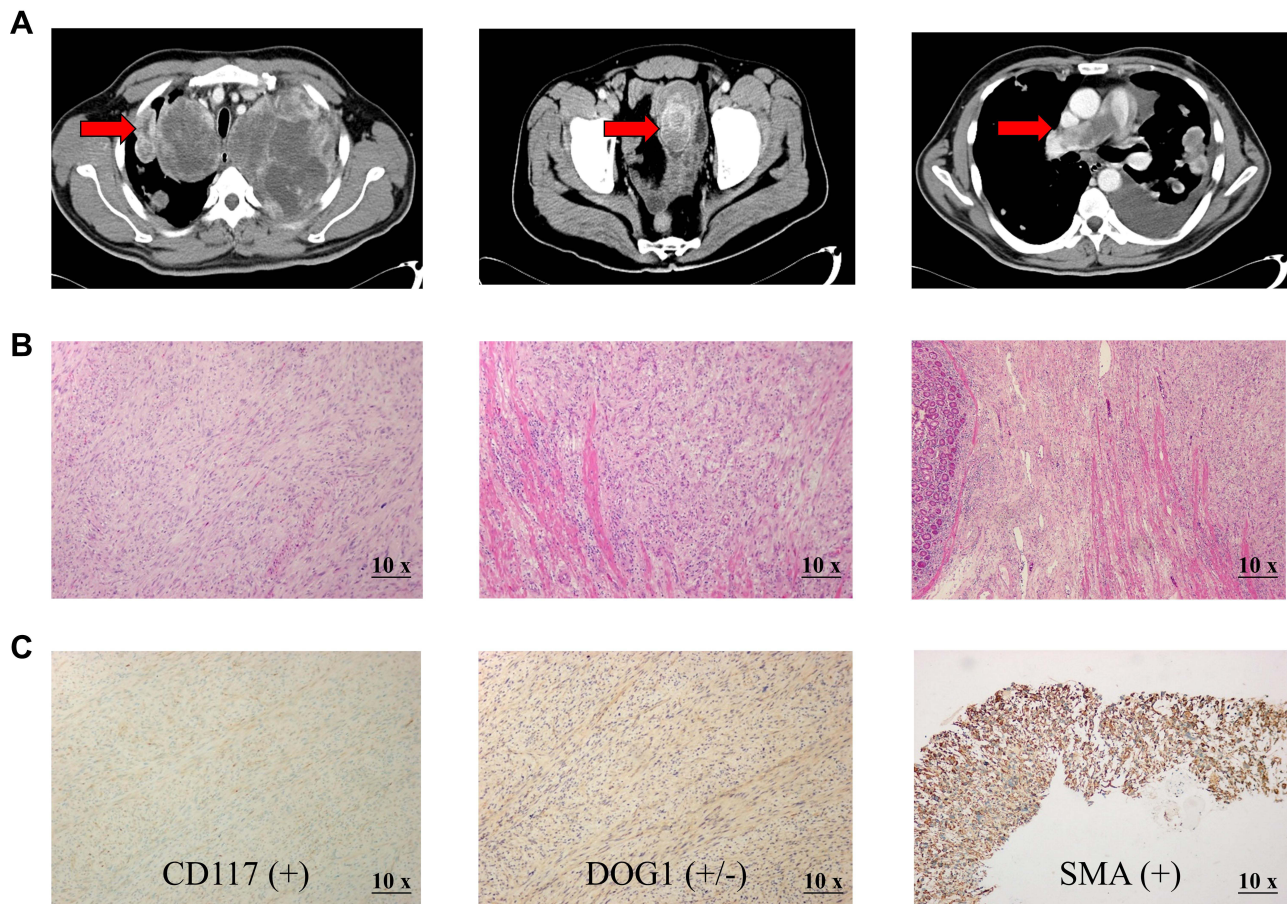


**Figure 1** Preoperative Contrast-enhanced CT images and postoperative histology examination of the LGMS specimen. **(A)**, CT images at the initial diagnosis (the lesions are indicated by arrows). **(B)**, The LGMS tumor cells are mainly in a fascicular arrangement, infiltrative growth with unclear boundaries, with light to moderate heteromorphic and mitotic image (magnification, ×10). **(C)**, Immunohistochemical examination shows positive staining for CD117, DOG1 and SMA (magnification, ×10).

Additionally, intussusception and jejunal masses were confirmed. No other primary or metastatic lesions were detected in any examination.

The patient underwent surgical resection of the jejunal mass on February 22, 2017. Histopathological results ([Figure 1B](#)) revealed that the tumor cells were composed of spindle-shaped cells arranged in sheet-like or storiform patterns. The nuclei of the tumor cells showed mild to moderate atypia. Mitotic rate averaged 4/high-power field (HPF). The immunohistochemical test results were as follows: DOG1 ( $\pm$ ), CD117 (+), SMA (+), desmin (-), and CD34 (-) ([Figure 1C](#)). Ki67 staining showed a proliferative index of 40% for neoplastic cells. After consultation with the Department of Pathology, Nanjing Medical University, the diagnosis of “low-grade myofibroblastic sarcoma with lung metastasis” was rendered.<sup>2,9,10</sup> To the best of our knowledge, this is the first case report of LGMS arising in the abdominal cavity with lung metastases.

Imatinib (400 mg/day) was given as the first-line treatment for one month, and liposomal doxorubicin (20 mg, day 1) and ifosfamide (1.8 g, day 1 to day 3, repeated every 21 days for two cycles) were administered as second-line chemotherapy for the next three months. CT revealed an obvious enlargement of the metastatic pulmonary tumor and qualified as progressive disease (PD) according to the modified RECIST criteria during the follow-up of the above treatment regimens. Subsequently, the patient was administered apatinib (500 mg) once daily. After two weeks of treatment, the symptoms of dyspnea were completely relieved. A CT scan indicated that the mass had observably decreased in size, achieving a partial response (PR) according to the modified RECIST criteria ([Figure 2A](#)). His serum CA125 level decreased significantly. During treatment with apatinib, the adverse event was a hand-foot syndrome (HFS) reaction. Therefore, apatinib was adjusted to 250 mg once daily, and toxicity was controllable and well tolerated. After four months of treatment with apatinib, CT showed that the size of the lung masses and mediastinal lymph nodes continued to decrease. At a follow-up of 8 months from the first month after apatinib treatment, serum CA125 levels remained within normal limits ([Figure 2B](#)), and CT images showed no recurrence. Yet after six months and 18 days after apatinib treatment, CT results showed that the tumor in both lungs increased, and new tumors appeared in the liver and pancreas. However, the patient refused to change his treatment plan and continued to receive apatinib. CT images taken on May 25, 2018 showed that the abdominal mass had grown. The patient decided to discontinue apatinib, and we provided him with the best supportive treatment. The patient died on July 26, 2018. Overall, this patient had a progression-free survival (PFS) of 8.5 months and an OS of 17 months.

## Whole-Exome Sequencing and RNA Sequencing Analysis

After obtaining consent from the patient’s family, the patient’s jejunal tumor and para-cancerous tissue samples (February 22, 2017) were subjected to WES and RNA-seq for further analysis in September 2018 ([Figure 3A](#)). Raw data were accessible through the EMBL-EBI database ERP120509 under the ENA, and the results were subjected to bioinformatics analysis.<sup>9</sup>

### Genomic Variation of LGMS

WES analysis revealed 256 genes involved in Single-nucleotide variations (SNV) ([Supplementary Table 1](#)). Classification was performed according to the variation type ([Figure 3B](#)), including missense mutations (95%), nonsense mutations (1%), splice sites (1%), frameshift mutations (1%), and inflame-del mutations (2%). According to the copy number variation (CNV) distribution in the chromosomes, of the 269 CNV genes, one gene was amplified and 265 were deleted ([Supplementary Table 2](#)). The CNV and SNP variation types and sites were plotted on high-resolution chromosome ideograms ([Figure 3C](#)). The location of mutations in the critical proteins MKI67, OR2J2, EPPK1, FCGBP, and OR10G4 is shown in [Figure 3D](#) and [E](#). These mutations are responsible for functional changes in the proteins ([Figure 3F](#)). Molecular docking was used to evaluate the binding ability between ligands and receptors, and based on the molecular docking model, we found that the mutated protein had a higher probability of docking with downstream genes than did the wild-type protein ( $E_{total} < 0$ , [Figure 3G](#)). These sites are considered to be mutational hotspots. A total of 93 risk subpathways were identified using the isubpathway Miner package ([Supplementary Table 3](#)). The three most significant subpathways were the PI3K-Akt, endocytosis, MAPK, and RIG-I-like receptor signaling pathways ([Figure 3H](#)).

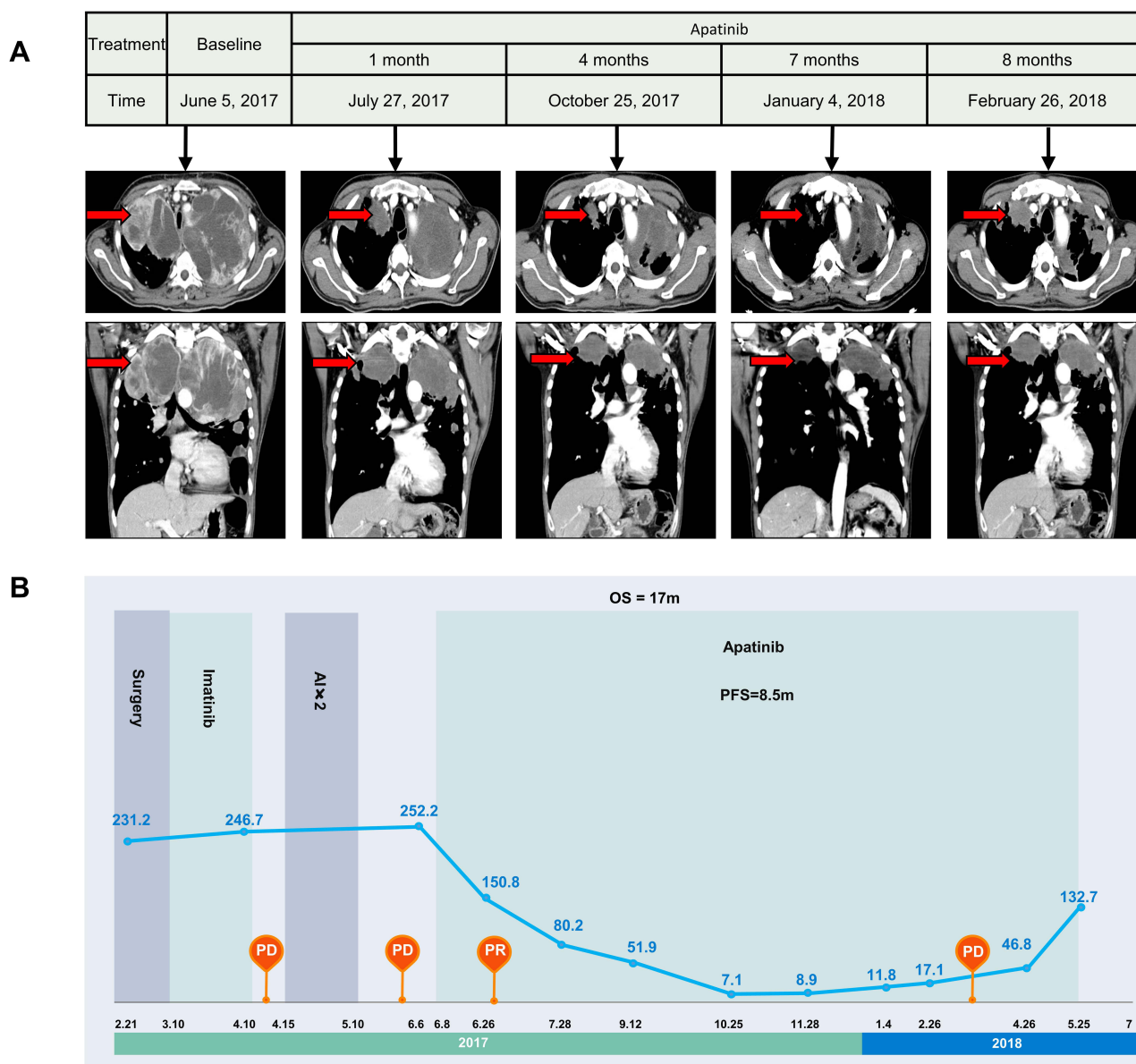


**Figure 2** Contrast-enhanced CT images and serum CA125 level changes throughout the apatinib therapy. **(A)** CT images reveal that the mass grew quickly until apatinib treatment was given. After apatinib treatment, the mass was observably decreases in size one month later and continues to shrink at a follow-up period of 4 months (October 25, 2017); however, the mass increases in size 7 months later (January 4, 2018), liver and pancreas metastasis are detected 8 months later (February 26 2018). **(B)** Serum CA125 levels continuously increase from 231.3 U/mL (February 21, 2017) to 252.3 U/mL (June 6, 2017) until apatinib treatment is given. After apatinib treatment begins in June 8, 2017, at a follow-up period of one month, serum CA125 levels significantly decrease to 150.8 U/mL (July 27, 2017). Then, apatinib is used as maintenance therapy, and CA125 dramatically decreases to a minimum of 7.1 U/mL (October 25, 2017). Finally, the evaluation indicates PD and the patient's CA125 increases to 132.7 U/mL again in May 25, 2018.

**Abbreviations:** PD, progressive disease; PR, response.

### Transcriptionally Characteristic of LGMS

In the LGMS sample, we screened 3311 differentially expressed genes (DEGs) (Supplementary Table 3) using RNA sequencing analysis, of which 1422 genes were upregulated and 1890 genes were downregulated (Figure 4A). Kyoto Encyclopedia of Genes and Genomes (KEGG) enrichment analysis revealed that the DEGs were mainly enriched in the PI3K signaling pathway, neuroactive ligand-receptor interaction signaling pathway, and cAMP signaling pathway (Figure 4B). Gene ontology (GO) analysis revealed that DEGs were significantly enriched in regulating extracellular structure organization, extracellular matrix organization, and humoral immune response mediated by circulating immunoglobulin (Figure 4C). Clue GO analysis suggested that cell signal transduction, surface receptor signal transduction

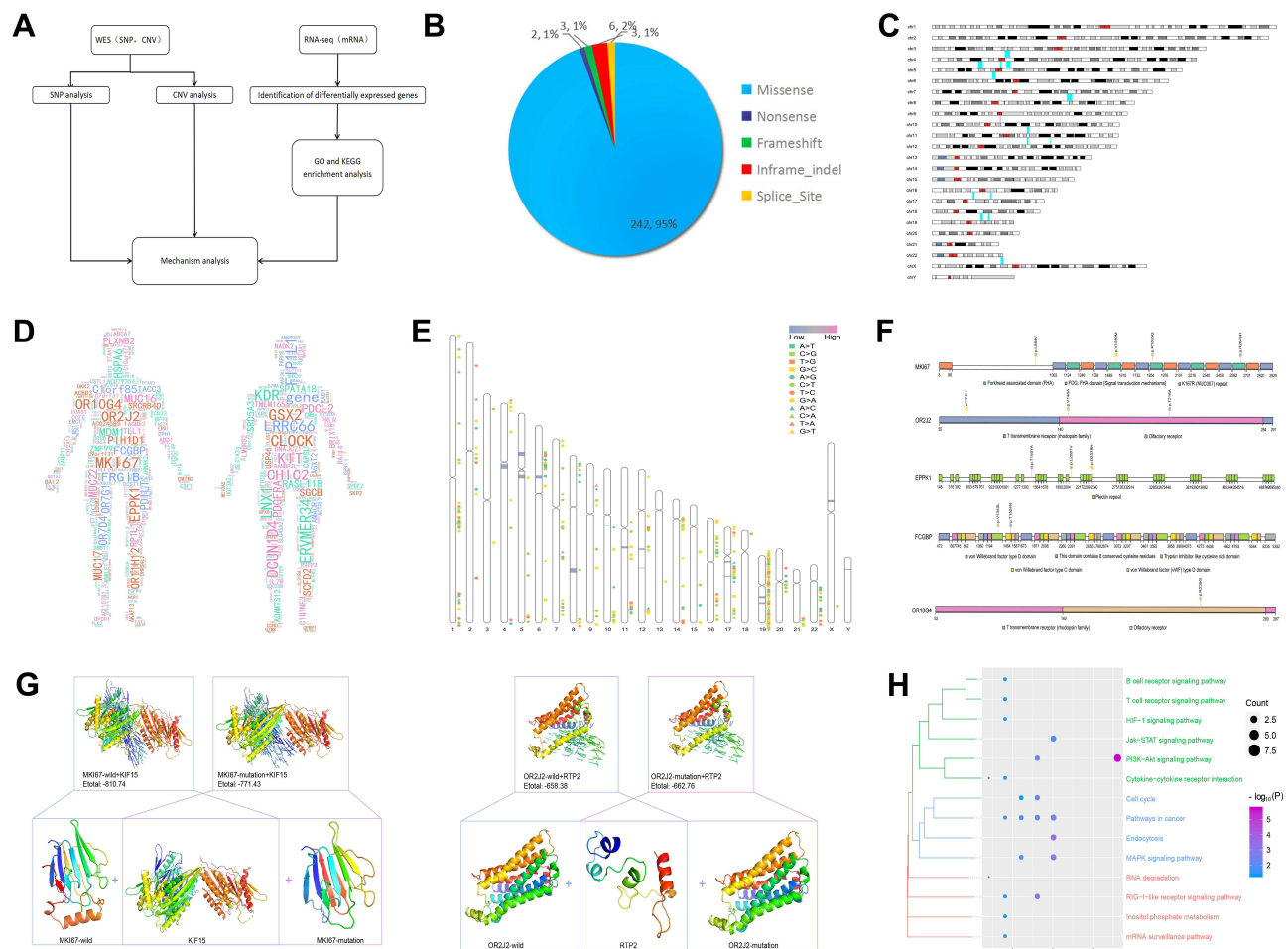


**Figure 3** The mutations detected by WES and RNA sequencing. **(A)** Framework of the bioinformatics analysis of the article. **(B)** The types of single-nucleotide variations. **(C)** The chromosomal locations of the copy number variations. The red fragment corresponds to the under-chromosome, which shows CNVs with amplification. In blue, CNVs with deletions are reported. **(D)** CNV and SNP of patients in the human body. Gene font size is directly proportional to the expression of CNV and SNP, and the color of the gene is random. **(E)** The distribution of CNV and SNP mutations sites are shown on a human chromosome ideogram. The different types of SNP mutations are annotated: red bar, amplification; blue bar, deletion. The chromosome number is indicated at the left of each ideogram. **(F)** Amino acid axis labels for domain start and stop positions, as well as exact marker locations, are clearly displayed for precision interpretation. **(G)** Visualization of the predicted chemical interaction between mutation genes. The 3D structure of the protein is modeled using Swiss MODEL. All the structural components of the protein including the C $\beta$ , all atoms, salvation and torsion angles were retrieved from Protein Data Bank (PDB) server. The visualization was drawn using PyMol. **(H)** Subpathway enrichment analysis of CNV and SNP mutation genes in LGMS patient ( $P < 0.05$ ).

pathway, and cell-cell adhesion through plasma membrane adhesion molecules were significantly enriched in the LGMS samples (Figure 4D).

## Discussion

### The Efficacy of LGMS Treatment and Prognosis

Patients with LGMS generally have good prognosis. Chan et al reported that the five-year overall survival rate of LGMS was 71.6% and the disease-specific survival rate was 76.3%.<sup>10</sup> Although, LGMS tends to recur locally, distant metastasis is occasionally observed.<sup>10</sup> The current mainstream view is that LGMS is not sensitive to radiotherapy and chemotherapy.<sup>11</sup> Yet, there have also been reports on the efficacy of chemotherapy and radiotherapy. Peng et al have reported that patients with LGMS in the pancreas after surgery and adjuvant chemotherapy have not relapsed for five years;<sup>7</sup> there is also a report of a patient with LGMS in the larynx who received postoperative radiotherapy and who was alive and disease-free for 14 months after the surgery<sup>12</sup> (Figure 5).

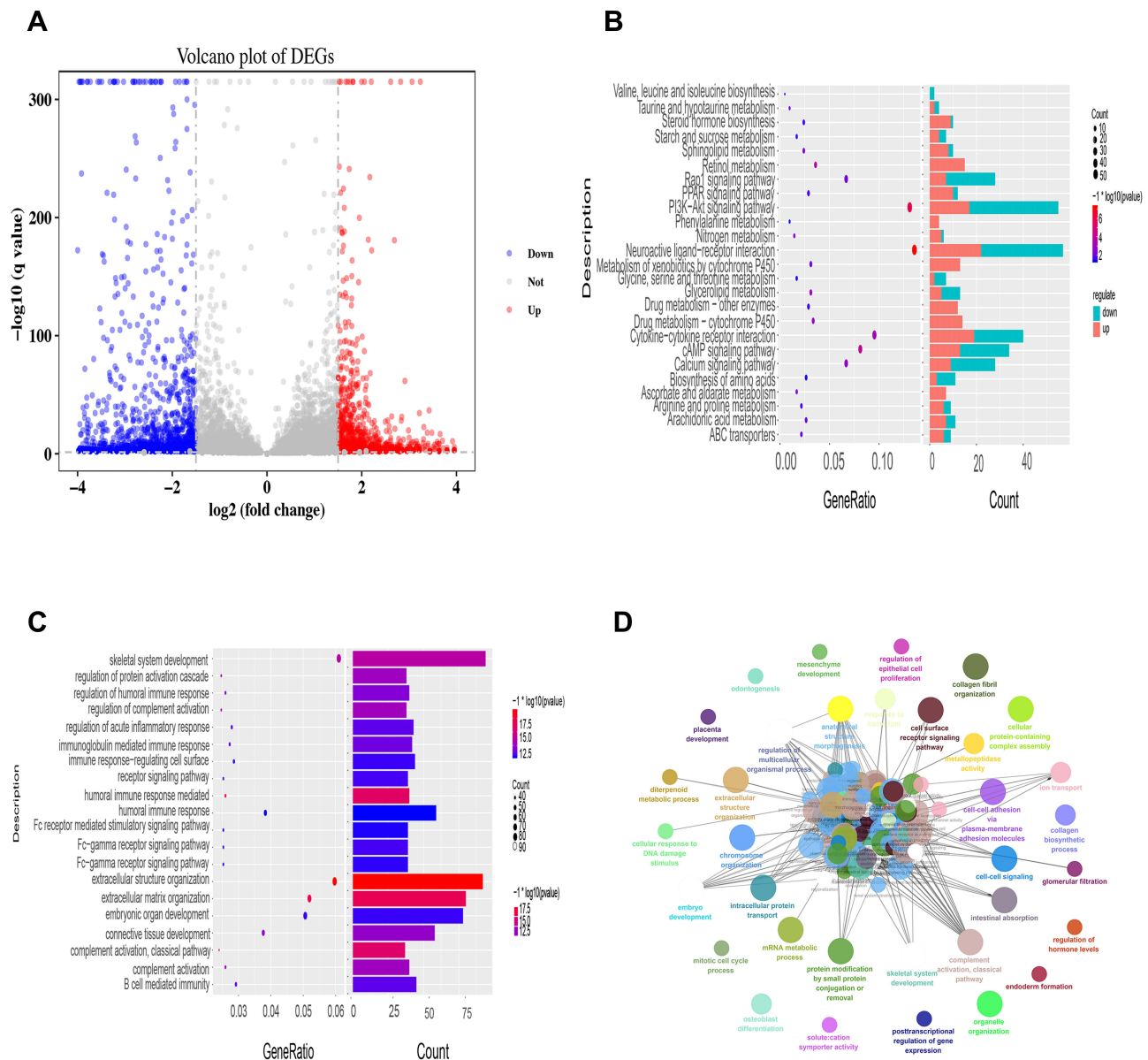


**Figure 4** Analyzing the potential mechanism and targets of LGMS by KEGG pathways and gene ontology. **(A)**, Volcanic map of the DEGs: The abscissa represents the  $\log_2FC$ , and the ordinate represents  $\log_{10}$  (adjusted P-value). Red dots, blue dots and gray dots show that the expression levels of the DEGs were obviously upregulated, downregulated, or had no significant difference, respectively. **(B)**, KEGG pathway analysis of LGMS. **(C)**, The biological processes of LGMS. **(D)**, GO (biological process) analysis was performed by Clue GO. Different colors of nodes refer to the functional annotation of ontologies. All these genes were discovered to be involved in 23 different biological processes.

## The Case and the Recurrence of LGMS

We reported a case of advanced LGMS that could not be resected by surgery R0. In our study, the patient was treated with imatinib, liposomal doxorubicin, and ifosfamide; however, CT revealed that the abdominal mass continued to grow. At the time, there was no standard second-line chemotherapy regimen for LGMS. The patient’s ECOG PS score indicated that his condition had deteriorated and he could not tolerate chemotherapy. After treatment with apatinib, CT showed that the size of the lung masses and mediastinal lymph nodes continued to decrease, and serum CA125 levels remained within normal limits. Overall, this patient had a PFS of 8.5 months and an OS of 17 months. The patient died of recurrence. In existing extensive reports on LGMS, recurrence is common.<sup>10,13</sup> The study reported a recurrence rate of 38% and a median recurrence time of 11.5 months.<sup>14</sup> Once recurrence appears, the prognosis is extremely poor. The mechanism of

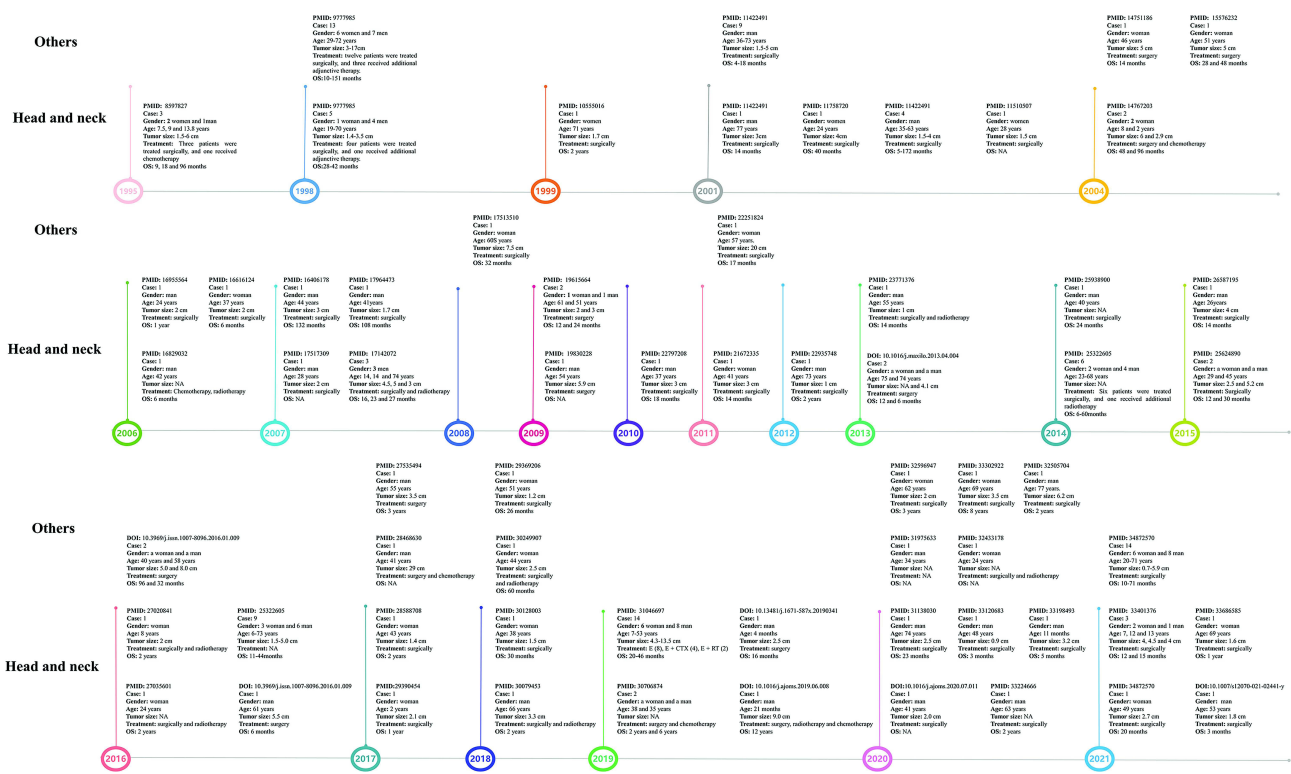


**Figure 5** Summary of the clinical features of previously reported LGMS cases.

recurrence has not been clarified and may be related to tumor size.<sup>14</sup> Furthermore, studies have shown by univariate analysis that local tissue infiltration and surgical methods are related to local recurrence.<sup>15</sup>

## VEGFR-PI3K/Akt Signaling Pathway May Be A Potential Target for Apatinib

The reason why apatinib treatment was effective may be related to the anti-tumor mechanism of apatinib and the result (PI3K-Akt pathway) in the bioinformatic analysis of LGMS patients.

Angiogenesis is essential for tumor growth and metastasis.<sup>16</sup> Vascular endothelial growth factor receptor (VEGFR) is a tyrosine kinase (TK) receptor and a key regulator of vascular endothelial growth factor. VEGFRs activate downstream signaling of the phospholipase C $\gamma$ -protein kinase CMAP kinase pathway but not the Ras pathway, leading to cell proliferation.<sup>16</sup> The VEGFR family includes three high-affinity TK receptors, namely Flt-1/VEGFR-1, Flk-1/KDR/VEGFR-2, and Flt-4/VEGFR-3,<sup>17</sup> which can promote tumor growth and metastasis and promote pathological angiogenesis. The TK activity of VEGFR-2 is much higher than that of VEGFR-1 and the VEGFR-3 system mainly regulates lymphangiogenesis.<sup>18</sup> Therefore, VEGFRs, especially VEGFR-2, are potential targets for tumor-targeted therapy. Specific targeting of VEGFR-2 inhibitors to inhibit VEGFR-2 activity is a potential strategy for inhibiting tumor angiogenesis. It has been confirmed that overexpression of the VEGFR family members, especially VEGFR-2, is significantly associated with a low survival rate in patients with sarcoma.<sup>19</sup> Vascular endothelial growth factor/vascular endothelial growth factor receptor is a targeted therapy for sarcoma because of its effect on angiogenesis and is often used to treat sarcoma.<sup>20,21</sup>

Apatinib can effectively inhibit VEGFR at very low concentrations, and higher concentrations can also inhibit platelet-derived growth factor receptor (PDGFR), c-Kit, c-Src, and other kinases. Apatinib can also inhibit the activity of VEGFR tyrosine kinase, block signal transduction after VEGF-VEGFR binding, and inhibit tumor angiogenesis. Preclinical studies have shown that apatinib can directly inhibit the VEGFR2-STAT3 signaling pathway and reduce the expression of PD-L1 in tumor cells.<sup>22,23</sup> In the report by Zhu et al, 31 patients with bone and soft tissue sarcoma were treated with apatinib, the clinical benefit rate was 75.0%, mPFS was 4.25 months, and mOS was 9.43 months;<sup>24</sup> Zhou

et al reported the efficacy of apatinib to a patient with osteosarcoma and lung metastasis, the PFS was 11 months;<sup>25</sup> Ji et al reported that a patient with advanced malignant fibrous histiocytoma was treated with apatinib for 2 cycles, and the lung metastasis obtained PR;<sup>26</sup> Li et al reported the efficacy of apatinib to 16 patients with advanced bone and soft tissue sarcoma, 2 patients obtained PR and mPFS reached 8.84 months;<sup>27</sup> Xie et al treated 55 sarcoma patients with apatinib (250–750 mg/d), and the results showed that the objective response rate (CR + PR) of osteosarcoma was 40.9%, that of Ewing's sarcoma was 70%, and that of cartilage The sarcoma was 100%, and the soft tissue sarcoma was 71.4%;<sup>23</sup> Liao et al treated patients with stage IV osteosarcoma (n=33) with apatinib for 12 weeks.<sup>19</sup> Clinical evaluation showed that two patients had PR, 24 patients had SD, seven patients had PD. The ORR, DCR, and PFR at 12 weeks were 6.06% (2/33), 78.79% (26/33), and 82%, respectively. At the end of the follow-up period, there were six cases of SD (18.18%, 6/33), 27 cases of PD (81.82%, 27/33), and 15 deaths (45.45%, 15/33). ORR was 0 (0/33), DCR was 18.18% (6/33), mPFS was 7.89 months (95% CI: 4.56–11.21). The mOS was 17.61 months (95% CI: 10.85–24.37).

The PI3K/Akt pathway is strongly associated with VEGFR expression. Studies have shown that VEGFR-2 is responsible for activating PI3K and Akt. In vitro experiments have shown that apatinib inhibits VEGFR-2-PI3K-Akt signal transduction by inducing intrahepatic cholangiocarcinoma cell apoptosis.<sup>28</sup> Similarly, in vitro experimental results show that apatinib can inhibit the migration and invasion of cholangiocarcinoma cells by inhibiting the VEGFR-2-dependent PI3K/Akt pathway.<sup>29</sup>

Moreover, the PI3K-Akt pathway is related to the efficacy of radiotherapy. Destroying the PI3K/Akt signaling pathway can inhibit DNA double-strand break repair and increase the sensitivity to radiotherapy.<sup>30</sup> A study has found that apatinib can enhance the efficacy of radiotherapy by inhibiting the PI3K/Akt signaling pathway in hepatocellular carcinoma.<sup>31</sup> This sheds light onto the potential treatment of LGMS. Perhaps, for LGMS patients with high PI3K/Akt expression, the combined use of apatinib and radiotherapy may have better efficacy.

## Limitations

Although the patient in this case was treated somewhat effectively with apatinib, this does not mean that apatinib is the only agent with a therapeutic effect. Other kinase inhibitors, such as pazopanib, a widely used multiple kinase inhibitor, can also inhibit VEGFR; however, owing to the lack of case-control studies, we could not assess its effects and mechanisms. In addition, the bioinformatics analysis results of only one patient cannot fully elucidate the problem, but they may provide a potential direction for future LGMS treatment.

## Conclusion

Our study indicated that apatinib may be an effective agent for treating LGMS. In the future, more prospective studies with larger numbers of patients are needed to explore comprehensive treatment regimens for LGMS.

## Abbreviations

LGMS, Low-grade myofibroblastic sarcoma; HCC, Hepatocellular carcinoma; WES, Whole-exome sequencing; RNA-seq, RNA sequencing; SNVs, Single-nucleotide variations; CNVs, Copy number variations; DEGs, Differentially expressed genes; GO, Gene Ontology; KEGG, Kyoto Encyclopedia of Genes and Genomes; PI3K, Phosphatidylinositol 3-kinase; ECOG PS, Eastern Cooperative Oncology Group performance status; HPF, High-power field; PD, Progressive disease; PR, Partial response; OS, Overall survival; HFS, Hand-foot syndrome; RFS, Recurrence-free survival; VEGF, Vascular endothelial growth factor; VEGFR-2, Vascular endothelial growth factor receptor-2; GBM, Glioblastoma multiform.

## Ethics Approval and Consent to Participate

This study was approved and supervised by the Clinical Research Ethics Committee of Guangxi Medical University Cancer Hospital. Written informed consent was obtained from the patient.

## Informed Consent

Written informed consent was obtained from the patient to publish their data.



## Consent for Publication

It is applicable for publication.

## Acknowledgments

We would like to thank Editage for English language editing. Yan Lin and Xing Gao are co-first authors for this study.

## Author Contributions

All authors made a significant contribution to the work reported, whether that is in the conception, study design, execution, acquisition of data, analysis, and interpretation, or in all these areas, took part in drafting, revising, or critically reviewing the article; gave final approval of the version to be published; have agreed on the journal to which the article has been submitted; and agree to be accountable for all aspects of the work.

## Disclosure

The authors declare that they have no competing interests in this work.

## References

1. Yonezawa H, Yamamoto N, Hayashi K, et al. Low-grade myofibroblastic sarcoma of the levator scapulae muscle: a case report and literature review. *BMC Musculoskelet Disord.* 2020;21(1):836. doi:10.1186/s12891-020-03857-3
2. Mentzel T, Dry S, Katenkamp D, Fletcher CD. Low-grade myofibroblastic sarcoma: analysis of 18 cases in the spectrum of myofibroblastic tumors. *Am J Surg Pathol.* 1998;22:1228–1238. doi:10.1097/0000478-199810000-00008
3. Maruyama T, Nakasone T, Nimura F, et al. Indolent growth of low-grade myofibroblastic sarcoma of the cheek mimics benign lesions: a case report and literature review. *Oncol Lett.* 2017;13:4307–4314. doi:10.3892/ol.2017.6020
4. Hou W, Su M, Li Q, Tian R. Low-Grade Myofibroblastic Sarcoma Demonstrated on 99mTc-MDP Bone Scan and 18F-FDG PET/CT. *Clin Nucl Med.* 2020;45:549–551. doi:10.1097/RLU.0000000000003073
5. Kuo YR, Yang CK, Chen A, Ramachandran S, Lin SD. Low-Grade Myofibroblastic Sarcoma Arising From Keloid Scar on the Chest Wall After Thoracic Surgery. *Ann Thorac Surg.* 2020;110:e469–469e471. doi:10.1016/j.athoracsur.2020.04.063
6. Miyazawa M, Naritaka Y, Miyaki A, et al. A low-grade myofibroblastic sarcoma in the abdominal cavity. *Anticancer Res.* 2011;31:2989–2994.
7. Peng L, Tu Y, Li Y, Xiao W. Low-grade myofibroblastic sarcoma of the pancreas: a case report and literature review. *J Cancer Res Ther.* 2018;14:S796–796S799. doi:10.4103/0973-1482.183551
8. Zhang S, Ma Y, Ma T, Wang Z. Low-grade myofibroblastic sarcoma of the orbit: a case report and literature review. *Medicine.* 2017;96:e9172. doi:10.1097/MD.00000000000009172
9. Gong J, Shao D, Xu K, et al. RISE: a database of RNA interactome from sequencing experiments. *Nucleic Acids Res.* 2018;46:D194–194D201. doi:10.1093/nar/gkx864
10. Chan JYK, Gooi Z, Wong EWY, Ng SK, Tong MCF, Vlantis AC. Low-grade myofibroblastic sarcoma: a population-based study. *Laryngoscope.* 2017;127(1):116–121. doi:10.1002/lary.26146
11. Von Mehren M, Randall RL, Benjamin RS, et al. Soft Tissue Sarcoma, Version 2.2018, NCCN Clinical Practice Guidelines in Oncology. *J Natl Compr Canc Netw.* 2018;16(5):536–563. doi:10.6004/jnccn.2018.0025
12. Yadav B, Kumar R, Ghoshal S, et al. Low-grade myofibroblastic sarcoma of the larynx: a rare entity with review of literature [J]. *J Cancer Res Ther.* 2013;9(2):284–286. doi:10.4103/0973-1482.113387
13. Tang L, Xu H, Gao H, Yang H, Chen S, Zhang P. Primary low-grade myofibroblastic sarcoma: a rare case report of this tumor in the orbit and literature review. *Eur J Ophthalmol.* 2020;1:1120672120970392. doi:10.1177/1120672120970392
14. Yamada T, Yoshimura T, Kitamura N, Sasabe E, Ohno S, Yamamoto T. Low-grade myofibroblastic sarcoma of the palate. *Int J Oral Sci.* 2012;4:170–173. doi:10.1038/ijos.2012.49
15. Kim JH, Choi W, Cho HS, Lee KS, Park JK, Kim BK. Surgical treatment and long-term outcomes of low-grade myofibroblastic sarcoma: a single-center case series of 15 patients. *World J Surg Oncol.* 2021;19:339. doi:10.1186/s12957-021-02454-5
16. Yoshida H, Yabuno A, Fujiwara K. Critical appraisal of bevacizumab in the treatment of ovarian cancer. *Drug Des Devel Ther.* 2015;9:2351–2358. doi:10.2147/DDDT.S83275
17. Shibuya M. Tyrosine Kinase Receptor Flt/VEGFR Family: its Characterization Related to Angiogenesis and Cancer. *Genes Cancer.* 2010;1:1119–1123. doi:10.1177/1947601910392987
18. Alitalo K, Carmeliet P. Molecular mechanisms of lymphangiogenesis in health and disease. *Cancer Cell.* 2002;1:219–227. doi:10.1016/s1535-6108(02)
19. Liao Z, Li T, Zhang C, et al. Clinical study of apatinib in the treatment of stage IV osteogenic sarcoma after failure of chemotherapy. *Cancer Biol Med.* 2020;17:501–512. doi:10.20892/j.issn.2095-3941.2019.0397
20. Zheng B, Ren T, Huang Y, Guo W. Apatinib inhibits migration and invasion as well as PD-L1 expression in osteosarcoma by targeting STAT3. *Biochem Biophys Res Commun.* 2018;495:1695–1701. doi:10.1016/j.bbrc.2017.12.032
21. Liu K, Ren T, Huang Y, et al. Apatinib promotes autophagy and apoptosis through VEGFR2/STAT3/BCL-2 signaling in osteosarcoma. *Cell Death Dis.* 2017;8:e3015. doi:10.1038/cddis.2017.422
22. Xie L, Xu J, Sun X, et al. Apatinib plus camrelizumab (anti-PD1 therapy, SHR-1210) for advanced osteosarcoma (APFAO) progressing after chemotherapy: a single-arm, open-label, Phase 2 trial. *J Immunother Cancer.* 2020;8. doi:10.1136/jitc-2020-000798

23. Xie L, Guo W, Wang Y, Yan T, Ji T, Xu J. Apatinib for advanced sarcoma: results from multiple institutions' off-label use in China. *BMC Cancer*. 2018;18:396. doi:10.1186/s12885-018-4303-z
24. Zhu B, Li J, Xie Q, Diao L, Gai L, Yang W. Efficacy and safety of apatinib monotherapy in advanced bone and soft tissue sarcoma: an observational study. *Cancer Biol Ther*. 2018;19:198–204. doi:10.1080/15384047.2017.1416275
25. Zhou Y, Zhang W, Tang F, et al. A case report of apatinib in treating osteosarcoma with pulmonary metastases. *Medicine*. 2017;96:e6578. doi:10.1097/MD.0000000000006578
26. Ji G, Hong L, Yang P. Successful treatment of advanced malignant fibrous histiocytoma of the right forearm with apatinib: a case report. *Oncotargets Ther*. 2016;9:643–647. doi:10.2147/OTT.S96133
27. Li F, Liao Z, Zhao J, et al. Efficacy and safety of Apatinib in stage IV sarcomas: experience of a major sarcoma center in China. *Oncotarget*. 2017;8:64471–64480. doi:10.18632/oncotarget.16293
28. Peng H, Zhang Q, Li J, et al. Apatinib inhibits VEGF signaling and promotes apoptosis in intrahepatic cholangiocarcinoma. *Oncotarget*. 2016;7:17220–17229. doi:10.18632/oncotarget.7948
29. Huang M, Huang B, Li G, Zeng S. Apatinib affect VEGF-mediated cell proliferation, migration, invasion via blocking VEGFR2/RAF/MEK/ERK and PI3K/AKT pathways in cholangiocarcinoma cell. *BMC Gastroenterol*. 2018;18:169. doi:10.1186/s12876-018-0870-3
30. Bussink J, van der Kogel AJ, Kaanders JH. Activation of the PI3-K/AKT pathway and implications for radioresistance mechanisms in head and neck cancer. *Lancet Oncol*. 2008;9:288–296. doi:10.1016/S1470-2045(08
31. Liao J, Jin H, Li S, et al. Apatinib potentiates irradiation effect via suppressing PI3K/AKT signaling pathway in hepatocellular carcinoma. *J Exp Clin Cancer Res*. 2019;38:454. doi:10.1186/s13046-019-1419-1

## Pharmacogenomics and Personalized Medicine

Dovepress

### Publish your work in this journal

Pharmacogenomics and Personalized Medicine is an international, peer-reviewed, open access journal characterizing the influence of genotype on pharmacology leading to the development of personalized treatment programs and individualized drug selection for improved safety, efficacy and sustainability. This journal is indexed on the American Chemical Society's Chemical Abstracts Service (CAS). The manuscript management system is completely online and includes a very quick and fair peer-review system, which is all easy to use. Visit <http://www.dovepress.com/testimonials.php> to read real quotes from published authors.

Submit your manuscript here: <https://www.dovepress.com/pharmacogenomics-and-personalized-medicine-journal>